

# Molecular sieving properties of the cytoplasm of *Escherichia coli* and consequences of osmotic stress

Jacek T. Mika, Geert van den Bogaart, Liesbeth Veenhoff, Victor Krasnikov and Bert Poolman\*

Department of Biochemistry, Groningen Biomolecular Science and Biotechnology Institute, Netherlands Proteomics Centre & Zernike Institute for Advanced Materials, University of Groningen, Nijenborgh 4, 9747 AG Groningen, the Netherlands.

## Summary

**We determined the diffusion coefficients (*D*) of (macro)molecules of different sizes (from ~0.5 to 600 kDa) in the cytoplasm of live *Escherichia coli* cells under normal osmotic conditions and osmotic upshift. *D* values decreased with increasing molecular weight of the molecules. Upon osmotic upshift, the decrease in *D* of NBD-glucose was much smaller than that of macromolecules. Barriers for diffusion were found in osmotically challenged cells only for GFP and larger proteins. These barriers are likely formed by the nucleoid and crowding of the cytoplasm. The cytoplasm of *E. coli* appears as a meshwork allowing the free passage of small molecules while restricting the diffusion of bigger ones.**

## Introduction

The cytoplasm of both eukaryotic and prokaryotic cells is a crowded environment with macromolecule concentrations as high as 200–300 g l<sup>-1</sup> for *E. coli* (Ellis, 2001; Cayley and Record, 2004). In such an environment the diffusion of particles is slower than in water. Increased crowding favours the association of (macro)molecules inside living cells and thus increases reaction rates (Ellis, 2001; Batra *et al.*, 2009). The crowding also slows diffusion of molecules, which will decrease reaction rates that are limited by diffusion. Because many biological reactions are often characterized *in vitro* at very low concentrations (hardly ever exceeding 10 g l<sup>-1</sup> and typically three

orders of magnitude lower), this may not reveal the reaction conditions present inside living cells (Ellis, 2001). It is thus important to have quantitative information on the equilibria of molecule associations, as well as the diffusion of low and high molecular weight molecules in the cytoplasm of live cells.

The measurements of diffusion in live bacteria by fluorescence recovery after photobleaching (FRAP)-based approaches are technically challenging due to the small size of the cells, which is only a few times bigger than the resolution of conventional light microscopy. Up to now there are few studies that address the mobility of macromolecules in bacterial cells (Elowitz *et al.*, 1999; Konopka *et al.*, 2006; 2009; Mullineaux *et al.*, 2006; van den Bogaart *et al.*, 2007; Slade *et al.*, 2009a,b; Kumar *et al.*, 2010). For GFP in the cytoplasm of *E. coli*, the diffusion coefficients are reported to be in the range of 3 to 10 μm<sup>2</sup> s<sup>-1</sup>, which compares with a value of about 90 μm<sup>2</sup> s<sup>-1</sup> in non-crowded, aqueous solution (Potma *et al.*, 2001).

Upon osmotic upshift *E. coli* cells instantaneously lose cytoplasmic water and eventually plasmolyze (Wood, 1999; Booth *et al.*, 2007). The loss of water results in a decrease of volume of the cytoplasm and an increase of (macro)molecule crowding, which may increase from 200–300 g l<sup>-1</sup> to 400 g l<sup>-1</sup> (Cayley *et al.*, 1991). This increased crowding translates to slowed diffusion in the cytoplasm (Konopka *et al.*, 2006; 2009; van den Bogaart *et al.*, 2007).

To the best of our knowledge the mobility of small molecules (less than 1 kDa) in the cytoplasm of live microbial cells has not been determined before. Also, it is not known to what extent an increased crowding as a result of osmotic stress influences the mobility of small versus big molecules. In this study, we investigate the consequences of osmotic stress by measuring the diffusion of (macro)molecules of different size. We observe that in osmotically stressed cells, both the nucleoid as well as the high crowding cause barriers for mobility. Most striking is that even at the highest osmotic upshifts (media supplemented with 2 M NaCl) small molecules of the size of metabolites remain fairly mobile and there are no apparent barriers limiting their diffusion. We discuss these findings in the light of our understanding of how bacteria recover from osmotic stress.

## Results

### Diffusion of macromolecules drops in osmotically upshifted cells

In this work, we refer to medium osmolalities as  $\Delta\text{LB}_{\text{Osm}}$ , that is, the osmolality relative to that of Luria Broth (LB), which has an osmolality of 0.44 Osm/kg. For microscopy measurements, the cells were placed in potassium-free NaPGCl (specified in the *Experimental procedures* section), which hindered cell recovery from osmotic upshifts. Inside cells, growing under normal osmotic conditions, proteins like GFP are evenly distributed throughout the cytoplasm (Konopka *et al.*, 2006; van den Bogaart *et al.*, 2007). When cells are transferred to a medium of higher osmolality than in which they were grown, the mobility of GFP decreases (Cayley *et al.*, 1991; Konopka *et al.*, 2006; van den Bogaart *et al.*, 2007). Figure 1 shows the time evolution of this phenomenon for an individual cell. For this purpose a microfluidic device (Rowat *et al.*, 2009) was used, which allows washing of the cells without affecting their position on the microscope slide. The cell was initially exposed to a medium isotonic with the growth medium ( $\Delta\text{LB}_{\text{Osm}} = 0$ ) and GFP fluorescence remained equally intensive in the entire cell. Upon photobleaching (Fig. 1, 1st purple arrow), the recovery of fluorescence was very fast (Fig. 1, after 1 min) and resulted in a uniform drop of fluorescence throughout the cytoplasm. When the cell was osmotically upshifted by exposing it to a medium supplemented with 1 M NaCl (Fig. 1, 3 min, white arrow) an instantaneous shrinking of the cytoplasm was observed. When the cell was now photobleached at the same position as before (Fig. 1, 2nd purple arrow), the recovery of fluorescence was relatively slow; even 2 min after bleaching, the fluorescence intensity at the bleaching spot was of lower intensity than that of the surrounding cytoplasm (Fig. 1, 5 min). However, diffusion was only slowed down and had not stopped completely, because after some time the bleached spot eventually recovered fluorescence (Fig. 1, 7 min).

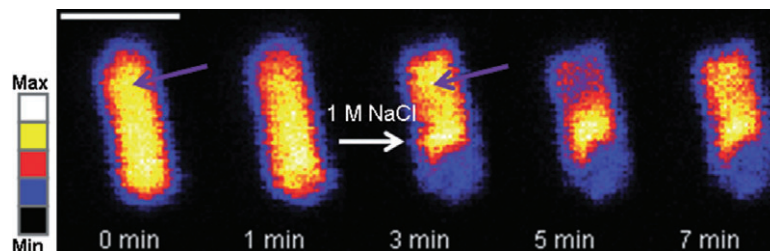


**Fig. 1.** Loss of macromolecule mobility in osmotically upshifted cells. *E. coli* cell in a microfluidic device and expressing GFP was imaged before and after osmotic upshift. Scale bar 2  $\mu\text{m}$ . Intensity is presented in rainbow setting (see scale). At  $t = 0$  min, the cell was under normal osmotic conditions ( $\Delta\text{LB}_{\text{Osm}} = 0$ ) and had a rod-like shape. Photobleaching (first purple arrow, at 0 min) resulted in uniform loss of fluorescence (1 min) owing to relatively fast GFP diffusion. When the cell was exposed to 1 M NaCl ( $\Delta\text{LB}_{\text{Osm}} = 1.65$ , white arrow), the cytoplasmic volume shrunk. Photobleaching at the same spot (3 min, second purple arrow) resulted in an initially non-uniform loss of fluorescence (5 min) and eventually a slow recovery of fluorescence (7 min). Microfluidic devices were handled as described (Rowat *et al.*, 2009).

### Consequences of osmotic upshift on cell structure

Under normal osmotic conditions ( $\Delta\text{LB}_{\text{Osm}} = 0$ ; Fig. 2), *E. coli* cells had a typical rod-like shape and GFP was evenly distributed throughout the cytoplasm (Fig. 2A, subpanel 1). Shifting cells to media of higher osmolality yielded more irregular and often rectangular-shaped structures. The extent of these changes was proportional to the severity of the osmotic upshift applied (Fig. 2A, subpanels 1 to 4). Significant structural perturbations (invaginations) could be observed in cells at  $\Delta\text{LB}_{\text{Osm}} = 0.85$  (Fig. 2A, subpanel 3), which have been referred to as visual plasmolysis spaces (Konopka *et al.*, 2006; 2009) and are considered as a hallmark of plasmolysis.

Severe osmotic upshifts caused heterogeneities in the cytoplasmic distribution of GFP. In a fraction of cells imaged ( $\sim 25\%$ ,  $n > 50$ ), the uneven distribution of GFP was so great that one could assign the areas to the nucleoid (Fig. 2B). These areas of the cytoplasm had a lower concentration of GFP, which co-localized with a region stained with the DNA-binding fluorophore Draq-5. In contrast to the non-stressed cells, GFP seemed partially excluded from the regions stained by Draq-5 (Fig. 2B, compare subpanels 1–3 vs. 5–7). Plotting the signal intensities originating from the GFP and Draq-5 (Fig. 2B, subpanels 3 and 7) reveals that in the osmotically stressed cells the nucleoid appears separated from the cytoplasm, which is not the case for cells in osmotic balance. Such a change in cellular substructure might imply a kind of phase separation of the nucleoid and the bulk of the cytoplasm, leading to a differential partitioning of macromolecules.

Subsequently, we investigated the effect of osmotic stress on the ultrastructure of the *E. coli* inner membrane, using LacY-GFP fusion as a reporter of the inner membrane. Under normal osmotic conditions, the inner membrane of *E. coli* formed a regular, ellipsoidal ring that borders the cytoplasm (Fig. 2B, panel 4). In osmotically upshifted cells, the inner membrane invaginated and formed irregular structures (Fig. 2B, panel 8).

### Barriers for mobility in osmotically shocked cells

Previously (van den Bogaart *et al.*, 2007), it was observed that the cytoplasm undergoes compartmentalization when the medium osmolality is increased by 0.5 M of salt or more. Pools of GFP were formed that did not exchange (or exchanged very slowly) their contents, indicating that the cytoplasm had lost continuity or developed a barrier for diffusion. The question is what is the molecular basis for the apparent compartmentalization? To address this point, *E. coli* cells expressing GFP were stained with Draq-5 and imaged. Subsequently, an area of cytoplasm adjacent to the nucleoid (but not the position of the nucleoid itself) was photobleached and a second image was recorded after 120 s (Fig. 3A). In control experiments, where cells were not exposed to osmotic stress, the photobleaching resulted in a uniform drop of fluorescence, irrespective of the position of the photobleaching laser beam. On the contrary, in cells exposed to osmotic stress, different overlapping ultrastructural phenotypes were observed. The three most extreme cases are depicted schematically in panel A of Fig. 3: (i) cells that did not form barriers for mobility, (ii) cells in which the nucleoid seemed to act as a barrier and (iii) cells in which the macromolecular crowding seemed to result in much slower diffusion.

The acquired data were visually inspected and the cells were classified according to the three most distinct phenotypes. It was not always possible to unambiguously assign the cells as mixed phenotypes were observed (about 30% of the cells). An example of a cell that does

not show visible diffusion barriers is shown in Fig. 3B. This phenotype was observed in 20% of the cells ( $n=40$ ). These osmotically upshifted cells could not be discriminated from non-stressed cells. The phenotype in which the nucleoid seems to form a barrier for diffusion (Fig. 3C) was observed in another 20% of the cells. In these cells, the photobleaching of GFP resulted in a homogenous loss of fluorescence in only a part of the cytoplasm, that is, the area where the laser beam was positioned but not the part on the opposite side of the nucleoid. This implies that the DNA forms a physical barrier for diffusion and the photobleached GFP cannot pass this barrier and mix with the non-photobleached GFP on the other side of the nucleoid. In the majority (60%) of the cells, the macromolecular crowding itself seemed to cause a significant decrease in mobility (Fig. 3D). Photobleaching of GFP in those cells did not result in uniformly distributed loss of fluorescence, nor did it cause the entire part of the cytoplasm delimited by the nucleoid to lose fluorescence. In these cells, the photobleached area was not larger than the size of the focused laser beam, indicating that the mobility of GFP was very restricted and hardly any diffusion was observed.

### Diffusion as a function of molecular weight in the *E. coli* cytoplasm

We used pulsed-FRAP (van den Bogaart *et al.*, 2007) to determine the diffusion constants of a fluorescently labelled glucose (NBD-glucose,  $M_r = 423$  Da), a medium

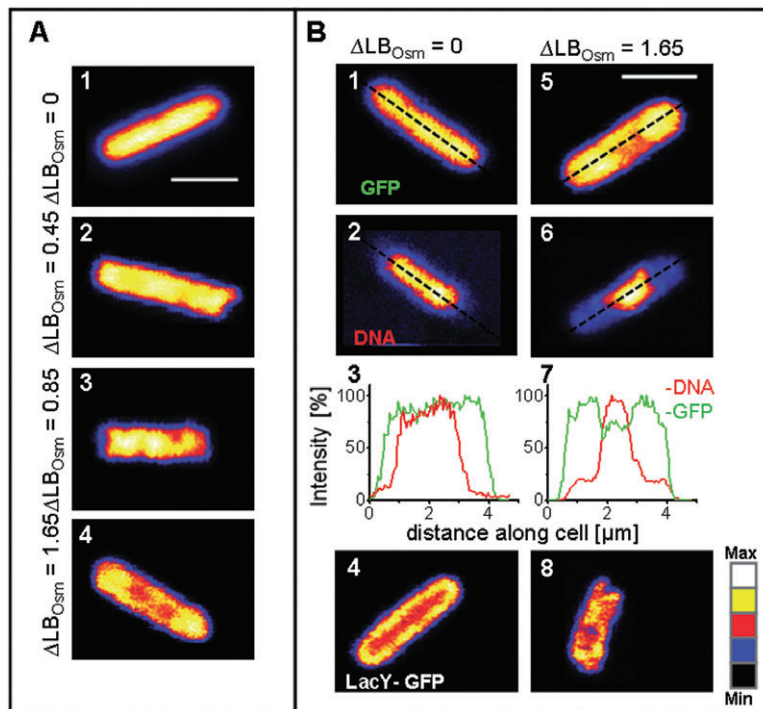


**Fig. 2.** Consequences of osmotic stress for the cell structure.

A. Cells expressing GFP: loss of the rod-like shape and uneven GFP distribution became more pronounced with increasing osmotic upshift (subpanels 1 to 4).

B. Comparison of cell structure under normal osmotic conditions (subpanels 1–4) and osmotic upshift (subpanels 5–8). Subpanels 1 and 5: cells expressing GFP. Subpanels 2 and 6: staining of DNA with Draq-5. Subpanels 3 and 7: fluorescence intensity distributions of the cross sections indicated in panels 1 and 5 (green; GFP) and 2 and 6 (red; DNA). Subpanels 4 and 8: images of cells expressing GFP-tagged LacY under normal osmotic conditions (4,  $\Delta LB_{Osm} = 0$ ) and osmotic upshift (8,  $\Delta LB_{Osm} = 1.65$ ). Scale bar 2  $\mu m$ . Intensity is presented in rainbow setting (see scale).

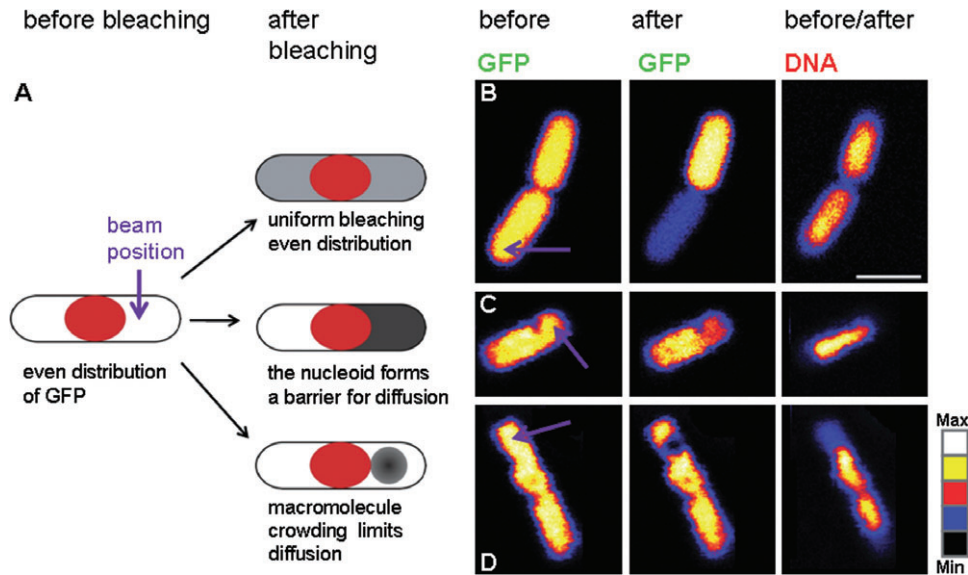


**Fig. 3.** Barriers for mobility in the cytoplasm of osmotically stressed *E. coli*.

A. Schematic representation of the phenotypes observed before and after osmotic upshift. The nucleoid is shown in red; GFP fluorescence intensity is shown in different shades of gray (from white, highest intensity, to dark gray, lowest intensity).

B–D. Cells expressing GFP (left images) and co-stained for DNA with Draq-5 (right images). The purple arrow indicates the location of the photobleached spot. Images: (B) A cell that does not seem to form barriers for mobility; (C) A cell where the nucleoid forms the barrier for mobility; (D) A cell where crowding forms the barrier for mobility. Scale bar 2  $\mu\text{m}$ . Intensity is presented in rainbow setting (see scale).

sized protein (GFP,  $M_r = 26.9$  kDa) and a large oligomeric protein consisting of four subunits of GFP-tagged  $\beta$ -galactosidase [ $(\beta\text{-gal-GFP})_4$ ,  $M_r \sim 582$  kDa]. Diffusion measurements were performed under non-stress and osmotic stress conditions and the data including spread of the measured values are summarized in Table S1; the distributions of the diffusion constants are indicated in Fig. S1. The diffusion constant of GFP in the cytoplasm of *E. coli* dropped with increasing osmotic stress as reported previously (Konopka *et al.*, 2006; 2009; van den Bogaart *et al.*, 2007). Moreover, the rates of diffusion could be restored by introducing osmoprotectants into the medium.  $D_{\text{median}}$  for GFP dropped from  $3 \mu\text{m}^2 \text{s}^{-1}$  to  $0.5 \mu\text{m}^2 \text{s}^{-1}$  when cells were exposed to 0.25 M NaCl ( $\Delta\text{LB}_{\text{Osm}} = 0.45$ ) and the  $D_{\text{median}}$  returned to  $1.5 \mu\text{m}^2 \text{s}^{-1}$  when the medium was supplemented with 10 mM KCl (Table S1). We were able to measure diffusion constants of GFP with pulsed-FRAP up to osmotic upshifts of 0.25 M NaCl. When the cells were subjected to larger osmotic stresses (0.5 M NaCl or more,  $\Delta\text{LB}_{\text{Osm}} = 0.85$ ), the photobleaching was not followed by instantaneous recovery and the diffusion coefficient could not be determined accurately. These cells underwent compartmentalization and GFP was essentially immobile with a  $D$  value estimated to be lower than  $0.001 \mu\text{m}^2 \text{s}^{-1}$ .

The decrease of diffusion as a function of molecular weight was determined (Fig. 4A); the diffusion median of NBD-glucose, GFP and  $(\beta\text{-gal-GFP})_4$  for cells under normal osmotic conditions was 50, 3 and  $0.8 \mu\text{m}^2 \text{s}^{-1}$

respectively (Table S1). The decrease in diffusion with increasing molecular weight was even more pronounced for osmotically stressed cells (Fig. 4B). The obtained decay of  $D$  as a function of molecular weight was fitted with the simple power dependence:

$$D_{\text{median}} = aM^{\text{exp}},$$

where  $M$  is the molecular weight of the diffusing molecule and  $a$ , a scaling constant. For cells under normal osmotic conditions the exponent was  $-0.7$  and for upshifted cells  $-0.8$ . The obtained fits clearly deviate from the Einstein–Stokes equation ( $D = aM^{-0.33}$ ; dashed line in Fig. 4A and B). It should be stressed that for the data analysis, the shape and density of the molecules were assumed to be similar; see Table S2 for details on the hydrodynamic radii of the molecules.

The dependencies of the diffusion coefficients of NBD-glucose and GFP as a function of salt stress are shown in Fig. 4C.  $D_{\text{median}}$  values for each osmotic upshift condition were divided by the corresponding values in aqueous media ( $D_0$ ). Clearly, the slope of diffusion decrease is steeper for GFP than for NBD-glucose as the medium osmolality increases. It is striking that even in cells upshifted with 2 M NaCl ( $\Delta\text{Osm} \sim 4.5$ ), NBD-glucose still remained mobile (Fig. 4C, Table S1) with a  $D_{\text{median}}$  of  $4.3 \mu\text{m}^2 \text{s}^{-1}$ , whereas GFP became essentially immobile with  $D$  values not exceeding  $0.001 \mu\text{m}^2 \text{s}^{-1}$  (Table S1). This implies that in plasmolyzing cells low molecular weight compounds (e.g. metabolites) still diffuse whereas

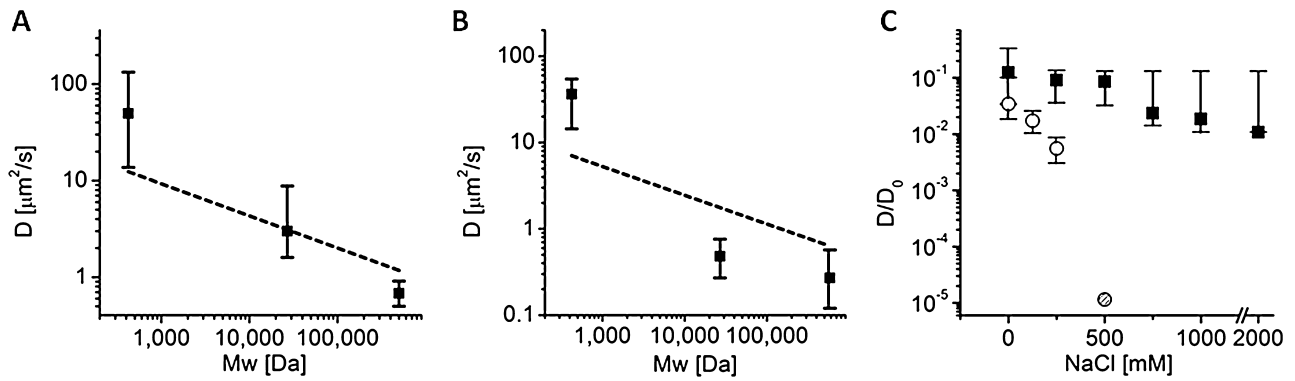


**Fig. 4.** Diffusion decreases with molecule size.

A. Median  $D$  values under normal osmotic conditions,  $\Delta LB_{Osm} = 0$ , as a function of molecular weight (Mw). The broken line represents the Einstein–Stokes relationship (see *Results* section).

B. Median  $D$  values under moderate osmotic upshift (B),  $\Delta LB_{Osm} = 0.45$ , as a function of molecular weight (Mw). The broken line represents the Einstein–Stokes relationship.

C. Diffusion coefficients *in vivo* normalized to those in water ( $D/D_0$ ) for NBD-glucose (squares) and GFP (circles). The filled data point for GFP at 0.5 M NaCl indicates that the value is an estimate. The error bars indicate the data spread. Interquartile range (IQR) values were taken (Table S1) and divided by  $D_0$  (Fig. 3C).

macromolecules (e.g. enzymes) are confined to a fixed position.

#### No barriers for diffusion of small molecules

To unambiguously show that, above-threshold values of osmotic stress, macromolecules like GFP lose mobility and are trapped in compartments, while small molecules can still probe the entire cytoplasmic space, we performed a dual-colour FRAP experiment. For simultaneous probing of the mobility of high (fluorescent proteins) and low molecular weight species (NBD-glucose) in the same cell, we substituted GFP with the red-shifted fluorescent protein mPlum (Wang *et al.*, 2004).

*Escherichia coli* cells expressing mPlum were loaded with NBD-glucose and exposed to different degrees of osmotic upshift. In the vast majority (92%,  $n = 24$ ) of osmotically stressed cells (addition of 0.5 M NaCl,  $\Delta LB_{Osm} = 0.85$ ), mPlum fluorescence did not recover after photobleaching, while NBD-glucose was distributed homogeneously along the cell (Fig. 5). Severe osmotic stress does not influence the continuity of the cytoplasm for low molecular weight species. The cytoplasm appears to act as a meshwork allowing small molecules to diffuse freely whereas macromolecules get trapped, possibly due to the porosity, constriction or density of the macromolecular meshwork or because they cannot transit the barriers of different compartments.

## Discussion

In this study, we have used pulsed-FRAP and confocal imaging to probe the mobility of molecules of different sizes in the cytoplasm of *E. coli* under normal osmotic

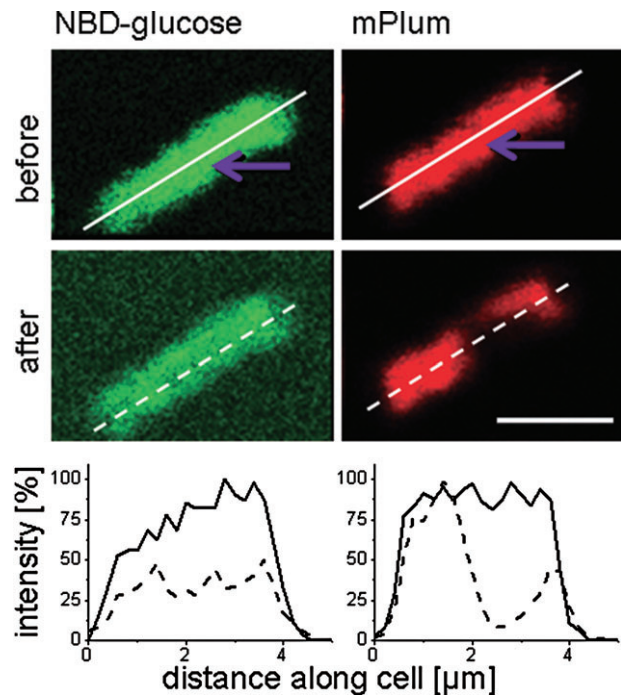


**Fig. 5.** The cytoplasm of osmotically upshifted cells forms mobility barriers for proteins (mPlum) but not for small molecules (NBD-glucose). Pseudo coloured images of an *E. coli* cell treated with 0.5 M NaCl ( $\Delta LB_{Osm} = 0.85$ ). Left panels, NBD-glucose (green) and right panels, mPlum (red). The purple arrow indicates the photobleaching spot. Upper panels show cells before, and lower panels 2 min after, photobleaching. The graphs indicate the normalized fluorescence intensities of the cell along the longer cell axis (white line through the cell) before (solid line) and after bleaching (dashed line). Scale bar 2  $\mu\text{m}$ .

conditions and hyperosmotic stress. We show that low molecular compounds can diffuse freely even in severely osmotically stressed cells, whereas proteins get trapped in subcompartments or become virtually immobile because of extreme crowding. Thus, owing to their high crowding, prokarya are readily impacted in their physiology upon osmotic challenge. Threshold values for mobility of macromolecules are reached even at moderate levels of osmotic stress.

#### Mobility of small molecules

The diffusion coefficient of NBD-glucose in the cytoplasm of live *E. coli* was  $50 \mu\text{m}^2 \text{s}^{-1}$ , which reflects a seven to eightfold reduction in mobility compared with aqueous solutions. The diffusion coefficient for NBD-glucose in water was around  $400 \pm 60 \mu\text{m}^2 \text{s}^{-1}$  (Table S2), which is similar to what has been reported for molecules of this size [e.g. Alexa fluor 488 is  $380 \mu\text{m}^2 \text{s}^{-1}$  at  $20^\circ\text{C}$  (Petrasek and Schwille, 2008)]. Kao and coworkers (Kao *et al.*, 1993) have probed the mobility of a small molecular weight dye BCECF in the cytoplasm of Swiss 3T3 fibroblasts. They reported a fourfold slower diffusion in the fibroblast cytoplasm than in diluted aqueous environments, which is consistent with our data as prokarya are more highly crowded than these eukaryotic cells (Ellis, 2001). We have tried to perform pulsed-FRAP measurements with this probe and observed that BCECF was not a suitable reporter of small molecule mobility in the cytoplasm of *E. coli* as the cells were not uniformly stained. Moreover, and consistent with our findings, BCECF has been reported to bind to other molecules in the matrix of mitochondria (Partikian *et al.*, 1998), resulting in very slow diffusion (Scalettar *et al.*, 1991).

#### Mobility of GFP

As reported previously (Elowitz *et al.*, 1999; Konopka *et al.*, 2006; Mullineaux *et al.*, 2006; van den Bogaart *et al.*, 2007) and confirmed here, translational diffusion of GFP in the cytoplasm of *E. coli* is an order of magnitude slower than in aqueous media. The  $D_{\text{median}}$  determined in this work is  $3 \mu\text{m}^2 \text{s}^{-1}$ , which is the same as reported previously (van den Bogaart *et al.*, 2007) and in reasonable agreement with values presented by others: 6, 7, 10 and  $12 \mu\text{m}^2 \text{s}^{-1}$  (in Elowitz *et al.*, 1999; Konopka *et al.*, 2006; 2009; Mullineaux *et al.*, 2006). The diffusion of GFP in the cytoplasm of eukaryotic cells, e.g. Swiss 3T3 fibroblasts and *Dictyostelium* cells, seems significantly higher with values of 27 and  $24 \mu\text{m}^2 \text{s}^{-1}$  respectively (Swaminathan *et al.*, 1997; Potma *et al.*, 2001).

#### Mobility of very large macromolecules

The  $D_{\text{median}}$  of the  $\sim 582$  kDa fusion protein ( $\beta\text{-gal-gfp}$ )<sub>4</sub> in the cytoplasm of *E. coli* was  $0.8 \mu\text{m}^2 \text{s}^{-1}$ , which is relatively

slow but is still significant because the molecules will traverse the cell several times each minute. About a decade ago, Elowitz *et al.* (1999) examined the mobility of this molecular species in *E. coli* cells and concluded that ( $\beta\text{-gal-gfp}$ )<sub>4</sub> was immobile. However, under their experimental conditions the fusion protein was not uniformly distributed throughout the cell. We believe that this indicates that the  $\beta$ -galactosidase moiety was not correctly folded, leading to large aggregates (inclusion bodies), which are immobile. We deliberately used a low inducer concentration (0.0002% w/v L-arabinose) and low temperature ( $30^\circ\text{C}$ ) to allow the multidomain fusion protein to fold correctly. Indeed, we observed uniform distribution of the protein throughout the cytoplasm in the vast majority of the cells ( $\sim 95\%$ ). Cells that showed signs of inclusion bodies were not used for the pulsed-FRAP measurements. We could reproduce the observations of Elowitz by expressing the protein at  $37^\circ\text{C}$  and using higher L-arabinose concentrations (0.02% w/v).

#### The cytoplasm a crowded meshwork

We observed different regimes in osmotic stress: (i) a moderate upshift ( $\Delta\text{LB}_{\text{Osm}} < 0.45$ ) resulted in a general decrease of mobility and (ii) a more severe osmotic upshift ( $\Delta\text{LB}_{\text{Osm}} \geq 0.85$ ) resulted in heterogeneities in the cytoplasm and introduced barriers for diffusion. Under these conditions, proteins of the size of GFP or bigger are no longer able to travel the entire cytoplasmic space. Dauty and Verkman (2004) studied the role of macromolecule crowding on the diffusion of differently sized macromolecules *in vitro* by elevating ficoll-70 concentration. The reduction in translational diffusion as a function of crowding was similar for molecules of different size. We observe that in live *E. coli* cells small molecules are slowed less than bigger ones, when the apparent crowding is increased by osmotic upshifts. In the cytoplasm of *E. coli* macromolecular structures of different size are present and the mobility is influenced by immobile obstacles (such as the nucleoid) or transient binding to cytoplasmic elements, which manifests itself in particular under conditions of hyperosmotic stress. In addition, translational diffusion of macromolecules seems to show a power-dependent drop with macromolecule size increase, but the observed decays substantially deviate from the Einstein–Stokes relationship, where the dependence of  $D$  on molecular weight (for globular-shaped molecules) has a cubic root dependence (Table S2). A similar finding was recently reported by others (Kumar *et al.*, 2010). The dependence of  $D$  on molecular weight obtained in this study can be used as a coarse approximation of the mobility of macromolecules in the cytoplasm of *E. coli*, for which no such data are available. The bacterial cytoplasm appears as a crowded mesh-

work in which intrinsic molecular species might get confined. As water leaves the cytoplasm the crowding of the cytoplasm increases and the meshwork becomes tighter, allowing NBD-glucose to diffuse through whereas macromolecules get trapped.

#### *Does the nucleoid form a barrier for mobility?*

The idea that the nucleoid would form the mobility barrier in highly stressed cells was introduced previously (van den Bogaart *et al.*, 2007; Konopka *et al.*, 2009). It was proposed that the inner membrane would come in physical contact with the bacterial nucleoid (van den Bogaart *et al.*, 2007). Konopka *et al.* (2009) suggested that the porosity of the nucleoid towards molecules of different size might vary with the extent of osmotic shock. In the light of our new measurements, we conclude that in osmotically stressed cells not only the nucleoid forms a barrier but that macromolecular crowding itself can contribute even more significantly to the slowing down of macromolecule diffusion, which might appear as formation of diffusion barriers. Importantly, formation of these apparent barriers is reversible.

#### *Consequences of retained mobility of NBD-glucose*

Under conditions of high osmotic stress ( $\Delta\text{LB}_{\text{Osm}} \geq 0.85$ ) the low molecular weight fluorophore (NBD-glucose) was still mobile and able to probe the entire cytoplasmic space. Although the diffusion of enzymes may have almost halted under these conditions, biochemical activity may continue as long as metabolites are still mobile. This implies that small, important metabolites such as pathway intermediates, ATP, signalling molecules and inorganic ions are available in the entire cytoplasm regardless of the strength of the osmotic stress. Most likely, osmoprotectants also diffuse rapidly and their omnipresence and fast redistribution from spots of uptake or synthesis helps the restoration of osmotic balance.

## Experimental procedures

#### *Strains, growth and expression of fluorescent proteins*

*Escherichia coli* K-12 strain MG1655 (Genotype: F<sup>-</sup> lambda<sup>-</sup> *ilvG*<sup>-</sup> *rfb*-50 *rph*-1 Serotype: OR:H48:K-) was grown at 37°C with vigorous shaking in LB medium [LB is 10 g l<sup>-1</sup> Bacto Tryptone (Becton Dickinson), 5 g l<sup>-1</sup> Yeast extract (Becton Dickinson) plus 10 g l<sup>-1</sup> NaCl (Merck)]. Where necessary the medium was supplemented with 100 µg ml<sup>-1</sup> ampicillin (Sigma). For the expression of fluorescent proteins, the cells were transformed with the following plasmids: pGFPCR [GFP (van den Bogaart *et al.*, 2007)], pBADmPlum (Wang *et al.*, 2004), pBAD-β-Gal-GFP (this work; yielding the β-galactosidase-gfp fusion protein) and LacY-GFP

(Geertsma *et al.*, 2008). Before the measurement a single colony was picked from a LB agar plate and a 4 ml culture was inoculated and grown to log phase ( $\text{OD}_{600} = 0.3\text{--}0.4$ ). The cultures were maintained in the exponential phase of growth by re-inoculation with fresh LB. Leaky expression of GFP from the pGFPCR plasmid was sufficiently high to allow measurements without inducing the cells. All other proteins were expressed from the arabinose promoter by supplementing the medium with 0.02% (w/v), 0.002% and 0.0002% L-arabinose (Sigma) for mPlum, LacY-GFP and (β-gal-gfp)<sub>4</sub> respectively. The expression of (β-gal-gfp)<sub>4</sub> and LacY-GFP was carried out at 30°C. The proteins were expressed and folded prior to the osmotic upshifts and microscopy measurements; as GFP is extremely stable the observed cellular fluorescence is due to the distribution of the protein rather than changes in its integrity.

#### *Preparation of the samples for microscopy*

Once the *E. coli* culture had reached an  $\text{OD}_{600} = 0.3\text{--}0.4$ , 1 ml of cells was taken and washed 2 times with NaPGCl medium (NaPGCl = 95 mM sodium phosphate, pH 7.0, 50 mM glucose plus 125 mM sodium chloride) which has an osmolality equal to that of LB ( $\Delta\text{LB}_{\text{Osm}} = 0$ ). For loading of the cells with NBD-glucose (Invitrogen), the glucose present in the medium was replaced with NaCl. The cells were then pelleted and resuspended in 50 µl of the same buffer. 2 µl of 10 mM NBD-glucose or 2.5 µl of 50 µM Draq-5 (Biostatus Limited) were added and the cells were labelled at 37°C with vigorous shaking for 20 min. After the labelling the cells were prepared for microscopy immediately. For measurements the cells were either kept in NaPGCl or osmotically upshifted by supplementing the media with NaCl. The osmolality of all solutions was measured by determination of the freezing point (Osmomat 030, Gonotec). For microscopy, 2 µl of cells was plated on poly-L-lysine (Sigma) coated cover slips (as described by (van den Bogaart *et al.*, 2007) and measurements were carried out immediately. Each sample was imaged for periods no longer than 25 min.

#### *Microscopy set-up, pulsed-FRAP measurements and data analysis*

The confocal microscope, diffusion measurements and data analysis were performed as described (van den Bogaart *et al.*, 2007), with the exception that diffusion constant medians were taken as the most representative mobility values instead of arithmetic means. For each osmotic condition, a minimum of 20 single cells was probed to determine the median diffusion constant. All measurements were performed at  $20 \pm 1^\circ\text{C}$ .

#### *Imaging of cells*

For imaging of cells expressing GFP or derivatives, or cells loaded with NBD-glucose, a 488 nm laser line was used with an emission filter of 500–600 nm. Draq-5 was excited with a 633 nm laser line and emission was detected between 650 and 700 nm. mPlum was excited with a 547 nm laser and

emission was collected between 600 and 700 nm. The laser intensity did not exceed 100  $\mu$ W at the back aperture of the objective. Cells were imaged within 25 min as described previously (Elowitz *et al.*, 1999; Konopka *et al.*, 2006; van den Bogaart *et al.*, 2007).

## Acknowledgements

We thank Amy Rowat at Harvard Medical School for supplying us with the microfluidic devices. We acknowledge financial support from SysMo via the BBSRC-funded KosmoBac programme coordinated by Ian R Booth (Aberdeen) and the NWO (Top-subsidy Grant 700.56.302).

## References

- Batra, J., Xu, K., Qin, S., and Zhou, H.Z. (2009) Effect of macromolecular crowding on protein binding stability: modest stabilization and significant biological consequences. *Biophys J* **97**: 906–911.
- van den Bogaart, G., Hermans, N., Krasnikov, V., and Poolman, B. (2007) Protein mobility and diffusive barriers in *Escherichia coli*: consequences of osmotic stress. *Mol Microbiol* **64**: 858–871.
- Booth, I.R., Edwards, M.D., Black, S., Schumann, U., and Miller, S. (2007) Mechanosensitive channels in bacteria: signs of closure? *Nat Rev Microbiol* **5**: 431–440.
- Cayley, S., and Record, M.T. (2004) Large changes in cytoplasmic biopolymer concentration with osmolality indicate that macromolecular crowding may regulate protein-DNA interactions and growth rate in osmotically stressed *Escherichia coli* K-12. *J Mol Recognit* **17**: 488–496.
- Cayley, S., Lewis, B.A., Guttman, H.J., and Record, M.T. (1991) Characterization of the cytoplasm of *Escherichia coli* K-12 as a function of external osmolarity. Implications for protein-DNA interactions in vivo. *J Mol Biol* **222**: 281–300.
- Dauty, E., and Verkman, A.S. (2004) Molecular crowding reduces to a similar extent the diffusion of small solutes and macromolecules: measurement by fluorescence correlation spectroscopy. *J Mol Recognit* **17**: 441–447.
- Ellis, R.J. (2001) Macromolecular crowding: obvious but underappreciated. *Trends Biochem Sci* **26**: 597–604.
- Elowitz, M.B., Surette, M.G., Wolf, P.E., Stock, J.B., and Leibler, S. (1999) Protein mobility in the cytoplasm of *Escherichia coli*. *J Bacteriol* **181**: 197–203.
- Geertsma, E.R., Groeneveld, M., Slotboom, D.J., and Poolman, B. (2008) Quality control of overexpressed membrane proteins. *Proc Natl Acad Sci USA* **105**: 5722–5727.
- Kao, H.P., Abney, J.R., and Verkman, A.S. (1993) Determinants of the translational mobility of a small solute in cell cytoplasm. *J Cell Biol* **120**: 175–184.
- Konopka, M.C., Shkel, I.A., Cayley, S., Record, M.T., and Weisshaar, J.C. (2006) Crowding and confinement effects on protein diffusion in vivo. *J Bacteriol* **188**: 6115–6123.
- Konopka, M.C., Sochacki, K.A., Bratton, B.P., Shkel, I.A., Record, M.T., and Weisshaar, J.C. (2009) Cytoplasmic protein mobility in osmotically stressed *Escherichia coli*. *J Bacteriol* **191**: 231–237.
- Kumar, M., Mommer, M.S., and Sourjik, V. (2010) Mobility of cytoplasmic, membrane and DNA-binding proteins in *Escherichia coli*. *Biophys J* **98**: 552–559.
- Mullineaux, C.W., Nenninger, A., Ray, N., and Robinson, C. (2006) Diffusion of green fluorescent protein in three cell environments in *Escherichia coli*. *J Bacteriol* **188**: 3442–3448.
- Partikian, A., Olveczky, B., Swaminathan, R., Li, Y., and Verkman, A.S. (1998) Rapid diffusion of green fluorescent protein in the mitochondrial matrix. *J Cell Biol* **140**: 821–829.
- Petrasek, Z., and Schwille, P. (2008) Precise measurement of diffusion coefficients using scanning fluorescence correlation spectroscopy. *Biophys J* **94**: 1437–1448.
- Potma, E.O., de Boeij, W.P., Bosgraaf, L., Roelofs, J., van Haastert, P.J., and Wiersma, D.A. (2001) Reduced protein diffusion rate by cytoskeleton in vegetative and polarized dictyostelium cells. *Biophys J* **81**: 2010–2019.
- Rowat, A.C., Bird, J.C., Agresti, J.J., Rando, O.J., and Weitz, D.A. (2009) Tracking lineages of single cells in lines using a microfluidic device. *Proc Natl Acad Sci USA* **106**: 18149–18154.
- Scalettar, B.A., Abney, J.R., and Hackenbrock, C.R. (1991) Dynamics, structure, and function are coupled in the mitochondrial matrix. *Proc Natl Acad Sci USA* **88**: 8057–8061.
- Slade, K.M., Baker, R., Chua, M., Thompson, N.L., and Pielak, G.J. (2009a) Effects of recombinant protein expression on green fluorescent protein diffusion in *Escherichia coli*. *Biochemistry* **48**: 5083–5089.
- Slade, K.M., Steele, B.L., Pielak, G.J., and Thompson, N.L. (2009b) Quantifying green fluorescent protein diffusion in *Escherichia coli* by using continuous photobleaching with evanescent illumination. *J Phys Chem B* **113**: 4837–4845.
- Swaminathan, R., Hoang, C.P., and Verkman, A.S. (1997) Photobleaching recovery and anisotropy decay of green fluorescent protein GFP-S65T in solution and cells: cytoplasmic viscosity probed by green fluorescent protein translational and rotational diffusion. *Biophys J* **72**: 1900–1907.
- Wang, L., Jackson, W.C., Steinbach, P.A., and Tsien, R.Y. (2004) Evolution of new nonantibody proteins via iterative somatic hypermutation. *Proc Natl Acad Sci USA* **101**: 16745–16749.
- Wood, J.M. (1999) Osmosensing by bacteria: signals and membrane-based sensors. *Microbiol Mol Biol Rev* **63**: 230–262.

## Supporting information

Additional supporting information may be found in the online version of this article.

Please note: Wiley-Blackwell are not responsible for the content or functionality of any supporting materials supplied by the authors. Any queries (other than missing material) should be directed to the corresponding author for the article.